Supporting Information for

Catalytic Reaction Mechanism of Acetylcholinesterase Determined by Born-Oppenheimer ab initio QM/MM Molecular Dynamics Simulations

Yanzi Zhou, Shenglong Wang, and Yingkai Zhang[*]

Department of Chemistry, New York University, New York, NY 10003 USA

* To whom correspondence should be addressed. E-mail: yingkai.zhang@nyu.edu

Computational Details

1. Preparation of initial enzyme reactant systems

The initial structure for investigating the acylation reaction stage was prepared similarly as in the previous study,[1] which was based on a snapshot of a 10-ns molecular dynamics simulation of the apo-mAChE (PDB code: 1MAH) with explicit water molecules.[2] The protonation states for all their titratable residues are in their normal states. First, we rotated the ring of His447 into its productive orientation. Then the AChE-ACh complex was constructed by docking the substrate acetylcholine (ACh) into the pre-equilibrated apo-AChE system using Autodock 4.0.1.[3] The partial charges of the ACh were fitted with HF/6-31G(d)[4] calculations and the restrained electrostatic potential (RESP) module[5] in the Amber package. Next, the system was neutralized, solved, and equilibrated with a series of minimizations interspersed by short molecular dynamics simulations using Amber10[6] with periodic boundary condition. Then an extensive molecular dynamics simulation was carried out and the trajectory is stable. A snapshot at 1.8 ns was randomly chosen for the subsequent QM/MM simulations.

For deacylation reaction, we prepared the initial structure from the computationally determined EA1 product of the acylation stage. We removed choline from the binding pocket since experimental studies have indicated that the release of choline is faster than the deacylation reaction[7,8]. In order to examine both possibilities for Glu202, we have prepared and simulated two reactant complex models for the deacylation stage, which only differ in the protonation state of Glu202. The rest equilibration and simulation protocol is the same as for the reactant of acylation reaction.

In all above MD simulations, long-range electrostatic interactions were treated with particle mash Ewald (PME) method[9,10] and 12 Å cutoff was used for both PME and van deer Waals (vdW) interactions. The pressure was maintained at 1 atm and coupled with isotropic position scaling.

Temperature was controlled at 298 K with Berendsen thermostat method.[11] They were performed with Amber10 molecular dynamic package,[6] and amber99SB[12,13] force fields was used.

2.2. QM/MM simulations.

With an equilibrated MD snapshot, the QM/MM model was prepared by deleting the ions and waters beyond 25 Å from the reaction center, which was chosen as hydroxyl oxygen atom of Ser203. Each resulted system contained about 10,000 atoms. For the acylation stage reaction, the QM sub-system includes the substrate ACh and the catalytic triad (side chains of Ser203, His447 and Glu334); while in the deacylation stage, the QM sub-system consists of the reactive water molecule and side chains of acetyl-Ser203, His447 and Glu334, as illustrated. The QM/MM boundary were described by improved pseudobond approach[14-17]. All other atoms were described by the same molecular mechanical force field used in classical MD simulations. For all QM/MM calculations, the spherical boundary condition was applied, and only the atoms within 20 Å from the reaction center were allowed to move. The 18 and 12 Å cutoffs were employed for electrostatic and van der Waals interactions, respectively. There was no cutoff for electrostatic interactions between QM and MM regions. The prepared QM/MM system was first minimized and then employed to map out a reaction path with B3LYP/6-31G* QM/MM minimizations. Figure S2 illustrates the reaction coordinate employed for each reaction step. For the initial step of acylation reaction, it is chosen as $d_{O\text{-}H} - d_{C\text{-}O}$, which is the distance between O-H bond of Ser203 and the distance between attacking O of Ser203 and the attacked carbon atom of ACh. It should be noted that the distance $d_{N\text{-}H}$ (distance between H of Ser203 and N of His447) is not included into the reaction coordinate, so that the proton is free to transfer either to His447 or to the O of scissile bond of ACh. Our simulations indicate that the proton doesn't transfer directly to the substrate. The reaction coordinate of the second acylation reaction step is $d_{C\text{-}O2} + d_{O\text{-}H} - d_{O2\text{-}H}$, in which $d_{C\text{-}O2}$ means the distance between C and O of the scissile bond, $d_{O2\text{-}H}$ is distance between H and the O atom of scissile bond. For the deacylation reaction, almost the same reaction coordinates have been employed. For the initial step of deacylation, we used reaction coordinate as $d_{O\text{-}H} - d_{C\text{-}O}$, which is the distance between O-H bond of reactive water and the distance between O of water to the attacked carbon atom of acyl-serine. For the second step, the reaction coordinate was chosen as $d_{C\text{-}O2} + d_{O\text{-}H} - d_{O2\text{-}H}$, in which $d_{C\text{-}O2}$ is the distance of scissile bond, and $d_{O2\text{-}H}$ is the distance between H and O of Ser203 respectively. For each determined structure along the path, a 500 ps MD simulation with MM force field was performed to equilibrate the MM subsystem, with the QM subsystem being frozen. Finally, the resulting snapshot was used as the starting structure for Born-Oppenheimer B3LYP/6-31G* QM/MM MD simulation with umbrella sampling. Along the reaction path, 11, 21, 13, 18 umbrella windows [18-20] were chosen for the two steps of acylation and deacylation respectively. Time step of 1 fs was employed, and the Berendsen thermostat method has been used to control the system temperature at 300 K. Each window was

simulated for at least 30 ps. From these biased simulations, the free energy profile for each reaction was obtained with the weighted histogram analysis method (WHAM).[21-23] All ab initio QM/MM calculations were performed with modified Q-Chem and Tinker programs.

References:

(1) Zhang, Y. K.; Kua, J.; McCammon, J. A. *J. Am. Chem. Soc.* **2002**, *124*, 10572-10577.

(2) Tai, K.; Shen, T. Y.; Borjesson, U.; Philippopoulos, M.; McCammon, J. A. *Biophys. J.* **2001**, *81*, 715-724.

(3) Morris, G. M.; Goodsell, D. S.; Halliday, R. S.; Huey, R.; Hart, W. E.; Belew, R. K.; Olson, A. J. *J. Comput. Chem.* **1998**, *19*, 1639-1662.

(4) Hehre, W.; Radom, L.; Schleyer, P.; Pople, J. *Ab Inition Molecular Orbital Theory*; John Wiley & Sons: New York, 1986.

(5) Wang, J. M.; Cieplak, P.; Kollman, P. A. *J. Comput. Chem.* **2000**, *21*, 1049-1074.

(6) Case, D. A.; Darden, T. A.; Cheatham, T. E.; III, C. L. S.; Wang, J.; Duke, R. E.; Luo, R.; Crowley, M.; Walker, R. C.; Zhang, W.; Merz, K. M.; Wang, B.; Hayik, S.; Roitberg, A.; Seabra, G.; Kolossváry, I.; K.F.Wong; Paesani, F.; Vanicek, J.; X.Wu; Brozell, S. R.; Steinbrecher, T.; Gohlke, H.; Yang, L.; Tan, C.; Mongan, J.; Hornak, V.; Cui, G.; Mathews, D. H.; Seetin, M. G.; Sagui, C.; Babin, V.; Kollman, P. A. University of California, San Francisco. , 2008.

(7) Froede, H. C.; Wilson, I. B.; Kaufman, H. *Arch. Biochem. Biophys.* **1986**, *247*, 420-423.

(8) Szegletes, T.; Mallender, W. D.; Thomas, P. J.; Rosenberry, T. L. *Biochemistry* **1999**, *38*, 122-133.

(9) Darden, T.; York, D.; Pedersen, L. *J. Chem. Phys.* **1993**, *98*, 10089-10092.

(10) Essmann, U.; Perera, L.; Berkowitz, M. L.; Darden, T.; Lee, H.; Pedersen, L. G. *J. Chem. Phys.* **1995**, *103*, 8577-8593.

(11) Berendsen, H. J. C.; Postma, J. P. M.; Vangunsteren, W. F.; Dinola, A.; Haak, J. R. *J. Chem. Phys.* **1984**, *81*, 3684-3690.

(12) Cornell, W. D.; Cieplak, P.; Bayly, C. I.; Gould, I. R.; Merz, K. M.; Ferguson, D. M.; Spellmeyer, D. C.; Fox, T.; Caldwell, J. W.; Kollman, P. A. *J. Am. Chem. Soc.* **1995**, *117*, 5179-5197.

(13) Hornak, V.; Abel, R.; Okur, A.; Strockbine, B.; Roitberg, A.; Simmerling, C. *Proteins: Structure, Function, and Bioinformatics* **2006**, *65*, 712-725.

(14) Zhang, Y. K. *Theor Chem Acc* **2006**, *116*, 43-50.

(15) Zhang, Y. K.; Lee, T. S.; Yang, W. T. *J Chem Phys* **1999**, *110*, 46-54.

(16) Zhang, Y. K.; Liu, H. Y.; Yang, W. T. *J Chem Phys* **2000**, *112*, 3483-3492.

(17) Zhang, Y. K. *J Chem Phys* **2005**, *122*, 024114.

(18) Patey, G. N.; Valleau, J. P. *J. Chem. Phys.* **1975**, *63*, 2334-2339.

(19) Roux, B. *Comput. Phys. Commun.* **1995**, *91*, 275-282.

(20) Boczko, E. M.; Brooks, C. L. *J. Phys. Chem.* **2007**, *97*, 4509–4513.

(21) Kumar, S.; Bouzida, D.; Swendsen, R. H.; Kollman, P. A.; Rosenberg, J. M. *J. Comput. Chem.* **1992**, *13*, 1011-1021.

(22) Souaille, M.; Roux, B. *Comput. Phys. Commun.* **2001**, *135*, 40-57.

(23) Ferrenberg, A. M.; Swendsen, R. H. *Phys. Rev. Lett.* **1988**, *61*, 2635-2638.

Figure S1. Illustration of the division of QM/MM system for a) acylation, b) deacylation reactions. All atoms colored in blue are assigned 6-31G* basis set, and the pseudo-atoms (colored in red) are treated with pseudo-bond parameters. All the left atoms are MM atoms that are treated with Amber99SB force field. The atoms connected with pseudo-atoms (colored in green) are treated as zero-charge atoms, and have no electrostatic interaction with QM atoms.

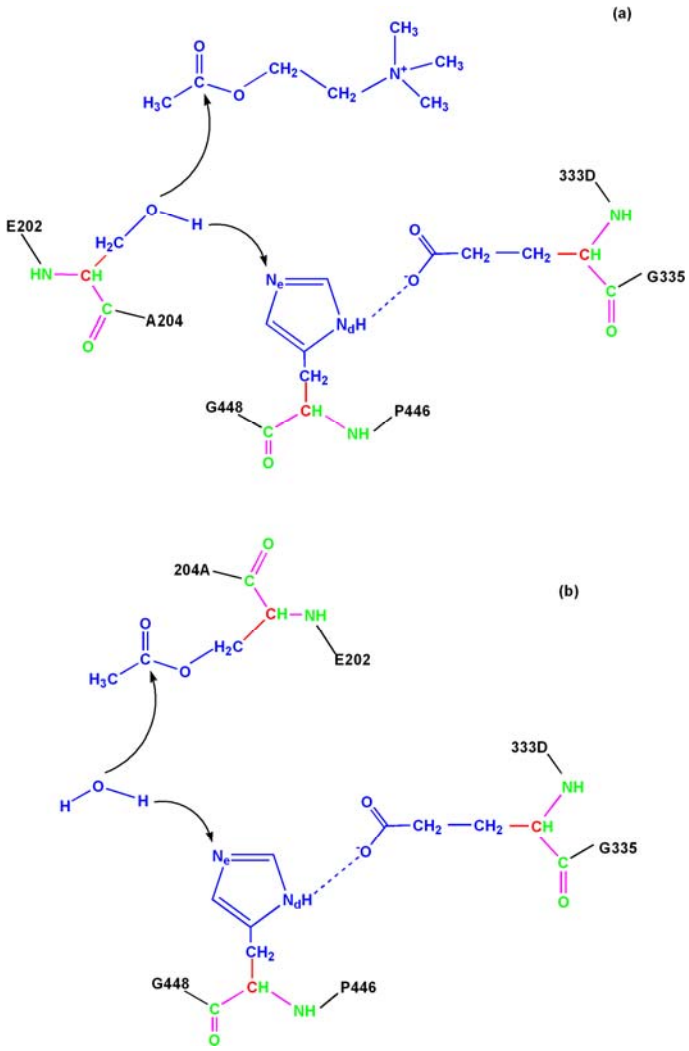

Figure S2. Illustration of reaction coordinate chosen for acylation and deacylation reactions: a) initial step of acylation, b) second step of acylatoin, c) initial step of deacylation, d) second step of deacylation.

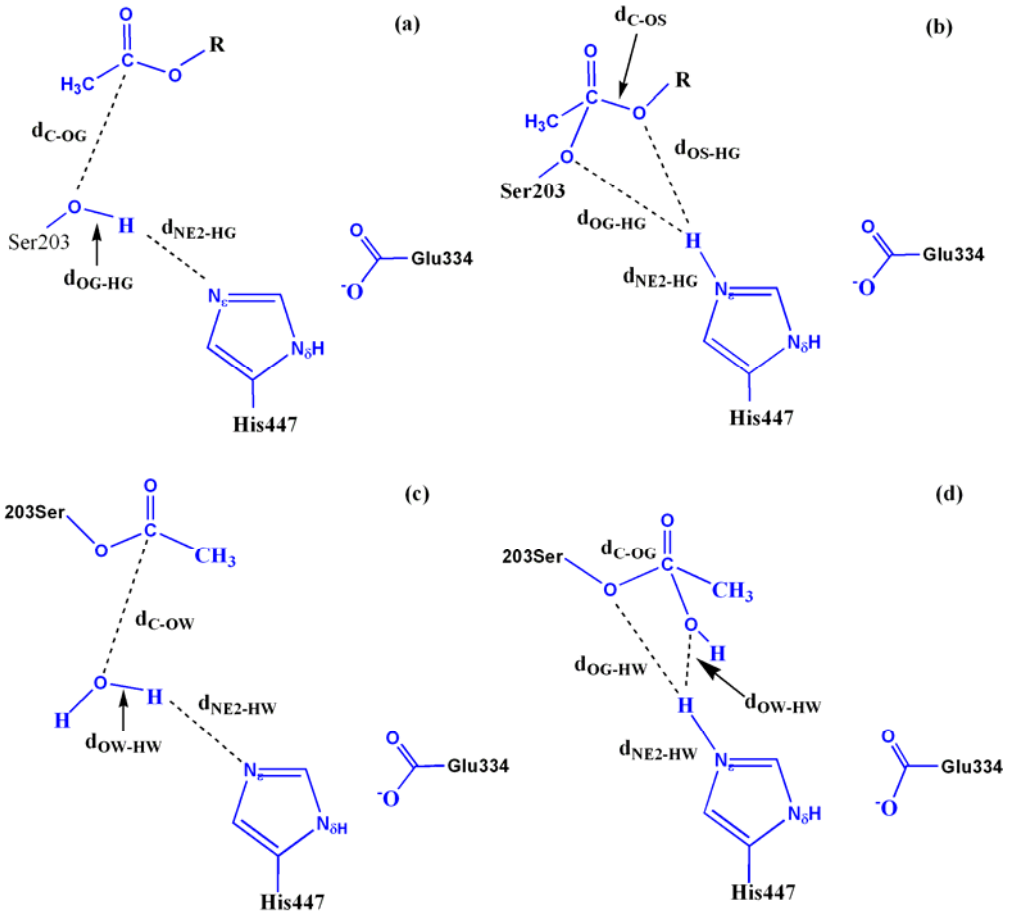

Figure S3. Free energy profile for the initial step of deacylation reaction with different protonation states of Glu202. The protonated Glu202 is referred as Glh202.

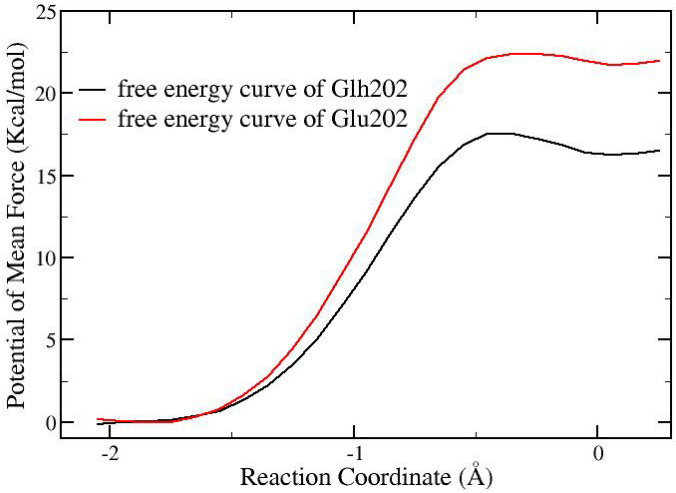

Figure S4. Free energy profile for the initial step of deacylation reaction with different functional and basis set with ab initio QM/MM MD simulations. The Glu202 is protonated. For B3lLYP/6-31+G(d)[1] QM/MM MD simulations, diffusion functions are only added on all the O ant N atoms.